Desalination and Water Treatment
www.deswater.com

doi:10.5004/dwt.2017.20956

82 (2017) 282–291
July

Removal of 2,4-dichlorophenoxy acetic acid from aqueous solutions by using activated carbon derived from olive-waste cake

Dilek Angin*, Ayşe Ilci

Department of Food Engineering, Faculty of Engineering, University of Sakarya, Esentepe 54187, Sakarya, Turkey, email: angin@sakarya.edu.tr, (D. Angin), a.ilci@hotmail.com (A. Ilci)

Received 27 July 2016; Accepted 16 May 2017

ABSTRACT

In this study, activated carbon was prepared from olive-waste cake by chemical activation using zinc chloride and subsequently it was utilized for the removal of 2,4-dichlorophenoxy acetic acid (2,4-D) from aqueous solution. The surface characterization of both raw material and activated carbon was undertaken byusing FTIR spectroscopy and scanning electron microscopy (SEM) technique. The surface area and micropore volume of chemically modified activated carbon were 1418 $m^2 g^{-1}$ and 0.197 $cm^3 g^{-1}$, respectively at 800°C and at an impregnation ($ZnCl_2$:olive-waste cake) ratio of 3:1. The adsorption experimental data indicated that the adsorption isotherms are well described by the Langmuir equilibrium isotherm equation and the calculated monolayer adsorption capacity was 129.87 mg g^{-1} at 298 K. The adsorption process attains equilibrium within 300 min and adsorption free energy is 0.707 kJ mol^{-1}. The adsorption kinetics of 2,4-dichlorophenoxy acetic acid (2,4-D) obeys the pseudo-second-order kinetic model. The thermodynamic parameters such as ΔG°, ΔH° and ΔS° were calculated to estimate the nature of adsorption and these parameters indicate a feasible, spontaneous and exothermic adsorption.According to these results, prepared activated carbon could be used as a low-cost and very effective adsorbent for the adsorption of 2,4-D from aqueous solutions.

Keywords: Olive-waste cake; Activated carbon; 2;4-Dichlorophenoxy-acetic acid; Adsorption

1. Introduction

2,4-Dichlorophenoxyacetic acid (2,4-D) is a typical chlorinated aromatic compound, which was first herbicide synthesized [1]. It is used for controlling wide variety of broad leaf weeds and grasses in plantation crops, such as sugar cane, oil palm, cocoa and rubber. The 2,4-D is commonly preferred because of its low-cost and good selectivity [1–3]. The World Health Organization identifies 2,4-D as moderately toxic (Class II) to human beings and animals and recommends the maximum permissible concentration in drinking water as 70 μg/L [1]. On the other hand 2,4-D is a poorly biodegradable pollutant. Consequently, it has been frequently detected in water bodies in various regions of the world. The toxicity of pesticides and their degradation products are making these chemical substances a potential hazard by contaminating our environment. Therefore, the removal of pesticides from water is one of the major environmental concerns [1–10].

Adsorption onto activated carbon is the most widespread technology used to remove toxic substances from wastewater due to its low cost, ease of operation, flexibility and simplicity of design [11–15]. Commercial activated carbon should have been a preferable adsorbent for the removal of organic pollutants from wastewater, but its widespread use is restricted due to high associated costs [16]. Therefore, many researchers have investigated more cheaper and efficient activated carbon production from industrial and agricultural wastes [16–21].

Food industries produce large volume of solid and liquid residues, which represent a disposal and potential environmental pollution problem. Likewise, olive oil production, one of the foremost agro-food industries in Mediterranean countries, generates different quantities and types of by products depending on the production system adopted

*Corresponding author.

Presented at the EDS conference on Desalination for the Environment: Clean Water and Energy, Rome, Italy, 22–26 May 2016

1944-3994 / 1944-3986

[22]. Turkey is the 6th in olive production in the world and according to FAOSTAT data olive and olive oil productions in the country were 1,700,000 and 190,000 tons, respectively, in 2015. Depending on the olive oil production method used in each country, amount of solid waste changes, e.g, in our country approximately 60–85% of solid waste is formed [23]. Therefore, this study has focused on the production and characterization of activated carbon from olive-waste cake by chemical activation with $ZnCl_2$. In addition, the adsorption of 2,4-dichlorophenoxyacetic acid (2,4-D) on activated carbon was studied with respect to pH, adsorbent dosage,contact times, solution temperature and initial 2,4-D concentration. The experimental data were analyzed by the Freundlich, Langmuir, Dubinin-Radushkevich and Temkin isotherms. Also, pseudo-first-order and pseudo-second-order kinetic models have been used to describe adsorption mechanism.

2. Materials and methods

2.1. Materials

Olive-waste cake was supplied by the HISAR Olive Ind. Inc. (Manisa, TURKEY), and they were first air dried, then crushed and finally sized. The fraction of particle sizes between 1 and 2 mm was chosen for subsequent studies. All chemical reagents used in this study were of analytical grade. 2,4-dichlorophenoxyacetic acid (2,4-D) with high purity (≥ 98%) was supplied from Sigma-Aldrich. The stock solution of 2,4-D was prepared by dissolving an accurate quantity of pesticide in deionized water.

2.2. Preparation of activated carbon

In the current study, chemical activation of olive-waste cake was performed using zinc chloride ($ZnCl_2$). The impregnation ratio was calculated as the ratio of the weight of $ZnCl_2$ in solution to the weight of the olive-waste cake used. The zinc chloride ($ZnCl_2$) impregnation ratio was selected as 3:1. Based on twenty to sixty grams of $ZnCl_2$ were dissolved in 250 mL of distilled water, and then twenty grams of olive-waste were mixed with the $ZnCl_2$ solution and stirred at approximately 80°C for 24 h to ensure a complete reaction between $ZnCl_2$ and olive-waste. The mixtures were then filtered and the remaining solids were dried at 105±3°C for about 24 h. Carbonization of the impregnated samples was carried out in a 316 stainless steel tubular reactor with a length of 90 mm and an internal diameter of 105 mm (Protherm PTF 12) under nitrogen flow (≈200 cm^3 min^{-1}) at heating rate of 10°C min^{-1} and held for 2 h at this final temperature. The resulting solids after carbonization were boiled at about 90°C with 100 mL of 1 N HCl solution for 30 min to leach out the activating agent, filtered and rinsed by warm distilled water several times until the pH value was reached to 6–7. Finally, they were dried at 105±3°C for 24 h.

2.3.Characterization of olive-waste cake and activated carbon

The contents of carbon, hydrogen, nitrogen and sulfur of the olive-waste cake and activated carbons were measured using a LECO CHNS 932 Elemental Analyzer with ±0.4% accuracy (LECO Instruments, USA). The oxygen contents were calculated by difference. Proximate analyses of olive-waste cake were determined according to the ISO R 771, ISO R 749 and ASTM E 872. Content of ash, moisture and volatile matter of activated carbon were determined according to the ASTM D2866, ASTM D2867 and ASTM D5832, respectively. Fixed carbon content was determined by difference. To determine the surface area of olive-waste cake and activated carbon, the nitrogen adsorption-desorption isotherms at 77 K were measured by an automated adsorption instrument, Micromeritics Instruments, Tristar II 3020. The surface area was determined from nitrogen adsorption data by using Micromeritics Instruments software. Adsorption data were obtained over the relative pressure, P/P_0, range from 10^{-5} to 1. The sample was degassed at 300°C under vacuum for 5 h. The apparent surface area of nitrogen was calculated by using the BET (Brunauer–Emmett–Teller) equation within the 0.01–0.2 relative pressure range. Surface functional groups of olive-waste cake and activated carbon were determined by Fourier transform infrared spectra (FTIR) using SHIMADZU IR Prestige 21. Also, surface morphologies were studied by scanning electron microscopy (SEM). SEM images were performed using JEOL-JSM-6060LV Scanning Electron Microscope.

2.4.Batch adsorption of 2,4-dichlorophenoxyacetic acid

Adsorption experiments were conducted through a batch type process. The studied variables were initial pH, adsorbent dosage and initial 2,4-D concentration of solution. In the procedure for the batch pH studies, 0.2 g adsorbent and 100 mL of 2,4-D solution containing 100 mg L^{-1} 2,4-D were mixed and shaken at 298 K for 24 h using a temperature controlled water bath with a shaker (GFL). After adsorption, samples were filtered and then the concentration of 2,4-D in the supernatant solution was analyzed. All concentrations were measured by using UV spectrophotometer (Shimadzu UV-Vis 1240) at 220 nm. The initial pH values of the solutions were adjusted to different values (2, 3, 5, 6.22, 7, 9 and 11) by adding dilute NaOH or HCl solutions. The pH was measured with pH-meter (Mettler-Toledo). After adsorption, the pH value providing the maximum 2,4-D removal was determined. Also, for the purpose of researched the effect of adsorbent dosage, batch experiments were carried out at 298 K and optimum pH value of the solution for 24 h shaking period by adding different amounts of activated carbon (0.1–0.8 g) into each 100 ml 2,4-D solution (100 mg L^{-1}). The removal percentage of 2,4-D was calculated according to the following equation:

$$\text{Removal}\ (\%) = \frac{C_0 - C_e}{C_0} \times 100 \quad (1)$$

where (mg L^{-1}) are initial and equilibrium concentrations of the pesticide (2,4-D), respectively [11,12,24].

For the adsorption isotherm and investigation of effect of initial concentration on 2,4-D removal, 0.2 g adsorbent was contacted with 100 mL 2,4-D solution with different initial concentration (50, 100, 150, 200, 250 and 300 mg L^{-1}) without adjusting pH (pH value 6.22). The flasks were agitated at 120 rpm using a temperature controlled water bath

with a shaker (GFL), and maintained at 298 K for 24 h until the equilibrium was reached. The suspensions were filtered and 2,4-D concentrations were measured using a UV spectrophotometer. 2,4-D uptake at equilibrium, q_e (mg g^{-1}), was calculated by the following equation:

$$q_e = \frac{(C_0 - C_e)V}{w} \tag{2}$$

where C_0 and C_e (mg L^{-1}) are initial and equilibrium concentrations of the 2,4-D, respectively, V (L) is the volume of the 2,4-D solution, and w (g) is the mass of used activated carbon [11–13]. The equilibrium data were then fitted using Langmuir, Freundlich, Dubinin-Radushkevick (D-R) and Temkin isotherm models.

Langmuir isotherm assumes monolayer adsorption onto a surface containing a finite number of adsorption sites. The linear form of Langmuir isotherm equation [11–16,25] is represented by the following equation:

$$\frac{q_e}{C_e} = \frac{1}{Q_0 K_L} + \frac{C_e}{Q_0} \tag{3}$$

where q_e is the equilibrium pesticide (2,4-D) concentration on the adsorbent (mg g^{-1}), C_e the equilibrium pesticide concentration in the solution (mg L^{-1}), Q_0 the monolayer adsorption capacity of the adsorbent (mg g^{-1}), and K_L is the Langmuir adsorption constant (L mg^{-1}). When C_e/q_e was plotted against C_e, straight line with slope $1/Q_0$ was obtained indicating that the adsorption of 2,4-D onto activated carbon.

The essential characteristics of the Langmuir isotherm can be expressed in terms of a dimensionless equilibrium parameter (R_L) which is defined by:

$$R_L = \frac{1}{1 + K_L \cdot C_0} \tag{4}$$

where K_L is the Langmuir constant and C_0 the highest pesticide (2,4-D) concentration (mg L^{-1}). The value of R_L indicates the type of the isotherm to be either unfavorable ($R_L > 1$), linear ($R_L = 1$), favorable ($0 < R_L < 1$) or irreversible ($R_L = 0$) [12,13].

Freundlich isotherm assumes heterogeneous surface energies, in which the energy term in Langmuir equation varies as a function of the surface coverage. The well-known logarithmic form of Freundlich isotherm is given by:

$$\log q_e = \log K_F + \frac{1}{n} \log C_e \tag{5}$$

where q_e is the amount adsorbed at equilibrium (mg g^{-1}), C_e the equilibrium concentration of the adsorbate (2,4-D), and K_F and n are Freundlich constants, n giving an indication of how favourable the adsorption process and K_F (mg g^{-1}) is the adsorption capacity of the adsorbent. K_F can be defined as the adsorption or distribution coefficient and represents the quantity of pesticide adsorbed onto activated carbon adsorbent for a unit equilibrium concentration. The slope *1/n* ranging between 0 and 1 is a measure of adsorption intensity or surface heterogeneity, becoming more heterogeneous as its value gets closer to zero. A value of $1/n$ below 1 indicates a normal Freundlich isotherm while *1/n* above 1 is indicative of cooperative adsorption [11–13,25].

The isotherm model suggested by Dubinin and Radushkevich [12,26] has been used to describe the liquid phase adsorption and on the basis of Dubinin–Radushkevich (D-R) equation adsorption energy can be estimated. Assuming that the adsorption in micropores is limited to a monolayer and the Dubinin–Radushkevich equation [12,27,28] can be written as:

$$q_e = q_s \exp\left(-B\varepsilon^2\right) \tag{6}$$

where q_s is the D-R monolayer capacity (mg g^{-1}), B a constant related to sorption energy, and ε is the Polanyi potential which is related to the equilibrium concentration as follows:

$$\varepsilon = \mathrm{RT} \ln\left[1 + \frac{1}{C_e}\right] \tag{7}$$

where R is the gas constant (8.314 J mol^{-1} K^{-1}) and T (K) is the absolute temperature. The constant B gives the mean free energy, E, of sorption per molecule of the sorbate when it is transferred to the surface of the solid from infinity in the solution and can be computed using the relationship:

$$E = \frac{1}{\sqrt{2B}} \tag{8}$$

The Temkin isotherm model [12,25,26] contains a factor that explicitly takes into account adsorbing species-adsorbate interactions. This model assumes the following: (i) the heat of adsorption of all the molecules in the layer decreases linearly with coverage due to adsorbent–adsorbate interactions, and that (ii) the adsorption is characterized by a uniform distribution of binding energies, up to some maximum binding energy. The derivation of the Temkin isotherm assumes that the fall in the heat of sorption is linear rather than logarithmic, as implied in the Freundlich equation. The Temkin isotherm has commonly been applied in the following form:

$$q_e = B_1 \ln\left(AC_e\right) \tag{9}$$

Eq. (9) can be linearized as:

$$q_e = B_1 \ln \mathrm{A} + B_1 \ln C_\mathrm{e} \tag{10}$$

where $B_1 = RT/b$, with b (J mol^{-1}), A (L g^{-1}), R (8.214 J mol^{-1} K^{-1}) and T (K) are Temkin constant related to heat of sorption, equilibrium binding constant, gas constant and absolute temperature, respectively [12,28].

Adsorption kinetic experiments were conducted by contacting 0.2 g adsorbent with 100 mL pesticide solution (100 mg L^{-1}) at 298 K solution temperature and optimum pH (6.22) with continuous shaking. The concentration of 2,4-D in supernatant was determined at different time intervals.

In order to analyze the kinetic mechanism of adsorption process, the experimental data were fitted in the pseudo-first-order, pseudo-second-order, and intra-particle diffusion models which are described as Eqs. (11)–(13);

Pseudo-first-order equation:

$$\log\left(q_e - q_t\right) = \log q_e - \frac{k_1 t}{2.303} \quad (11)$$

Pseudo-second-order equation:

$$\frac{t}{q_t} = \frac{1}{k_2 q_e} + \frac{t}{q_e} \quad (12)$$

Intra-particle diffusion equation:

$$q_t = k_p t^{\frac{1}{2}} + C \quad (13)$$

where q_t and q_e (mg g^{-1}) are amounts of 2,4-D adsorbed over a given period of time t and at equilibrium, respectively; t is the adsorption time (min); k_1 (min^{-1}), k_2 (g mg^{-1} min^{-1}), and k_p (mg g^{-1} min$^{-1/2}$) are the adsorption rate constant of the pseudo-first-order adsorption, the pseudo-second-order adsorption and the intra-particle diffusion,respectively; and C (mg g^{-1}) is a constant in the intra-particle diffusion equation, corresponding to the thickness of boundary layer [29–31].

Three thermodynamic parameters, i.e. change in the Gibbs free energy ($\Delta G°$), enthalpy ($\Delta H°$), and entropy ($\Delta S°$), were calculated to evaluate the thermodynamic feasibility and the nature of the adsorption process. $\Delta G°$ can be calculated according to the following equation:

$$\Delta G^o = -RTlnK_L \quad (14)$$

where R is the gas constant (8.314 J mol^{-1} K^{-1}), T is the temperature (K), and K_L is the thermodynamic equilibrium constant of the adsorption process, reflecting pesticide distribution between the solid and liquid phases at equilibrium. Equilibrium constant (K_L) was estimated as:

$$K_L = \frac{q_e}{C_e} \quad (15)$$

According to the van't Hoff equation:

$$\ln K_L = \frac{\Delta S^o}{R} - \frac{\Delta H^o}{RT} \quad (16)$$

The values of $\Delta H°$ (kJ mol^{-1}) and $\Delta S°$ (J mol^{-1}K^{-1}) were evaluated from the slope and intercept of van't Hoff plots [29,32].

3. Results and discussion

3.1. Characterization of olive-waste cake and activated carbon

The results of proximate and ultimate analysis and surface properties of the olive-waste cake and activated carbon are given in Table 1. The carbon content has increased by 77% relative to raw material after activation process which was determined as 87.92 wt.%. On the other hand, hydrogen, nitrogen and oxygen contents decreased. This is due to the release of volatiles during carbonization that results in the elimination of non-carbon species and enrichment of carbon [12,17]. Since the sulfur content of activated carbon was below the detection limit, the activated carbon could be used in adsorption and purification process.

Table 1
Characteristics of the olive-waste cake and activated carbon

Surface properties	Olive-waste cake	Activated carbon
BET surface area (m^2 g^{-1})	n.d.	1418.0
Micropore area (m^2 g^{-1})	n.d.	392.43
Total pore volume (cm^3 g^{-1})	n.d.	0.410
Micropore volume (cm^3 g^{-1})	n.d.	0.197
Average pore diameter (nm)	n.d.	1.16
Moisture content (wt.%)	4.66	1.40
Proximate analysis (wt.%)		
Volatile Matter	76.08	5.81
Ash	3.56	0.22
Fixed carbon*	20.36	93.97
Ultimate properties		
Carbon	49.55	87.92
Hydrogen	6.55	1.14
Nitrogen	0.38	0.54
Sulphur	n.d.	n.d.
Oxygen*	43.52	10.40

*By difference
* n.d.: not determined

The olive-waste cake contains 3.56 wt.% ash, 76.08 wt.% volatile matter and 20.36 wt% fixed carbon. The acceptable ash content of the olive-waste cake indicates that it is a suitable precursor for activated carbon production. The activation process led to an increase in fixed carbon content while decreasing in volatile matter content. The content of ash was greatly decreased. This is due to the release of volatiles during carbonization that results in the elimination of non-carbon species and enrichment of carbon [33]. The porosity has a strong effect on the adsorption properties of the activated carbon. The specific surface area of activated carbon was found to be 1418 m^2 g^{-1} and the most of the material (28%) consist of micropores. The activated carbon produced from olive-waste cake in this study contained both micropores and mesopores but the mesopore volume was larger than the micropore volume.

Even though the identification of all the chemical species on the surface of a chemically modified ($ZnCl_2$) activated carbon is not an easy task: however, the information about the chemical nature of the carbon surfaces may be obtained by using Fourier transform infrared (FTIR) spectroscopy. FTIR analysis results of olive-waste cake and activated carbon were given in Fig. 1. The O–H stretching vibrations between 3200 and 3400 cm^{-1} of the precursor material (olive-waste cake) indicate the presence of phenols and alcohols. The low frequency values for these bands suggest that hydroxyl groups are involved in hydrogen bonds [34,35]. The binary band appearing in the FTIR spectrum at about 2922.87 cm^{-1} were generally attributed to symmetric or asymmetric stretching of aliphatic band in –CH, –CH_2 or –CH_3 [21]. This band was observed as much stronger at olive-waste cake than activated carbon. These two func-

tional groups were formed, possibly due to the extraction of H element and OH groups from the aromatic rings during the impregnation and heat treatment stages as a result of the dehydration effect of $ZnCl_2$ [36]. Also the presence of the above mentioned peaks together with the presence of C=O stretching vibrations between 1700 and 1750 cm^{-1} is compatible with the presence of ketone and aldehyde groups. The presence of both O–H and C=O stretching vibrations also indicated the presence of carboxylic acids and their derivatives [34]. This carbonyl and carboxyl groups are also preserved in activated carbon obtained after heat treatment. The peak 1031.15 cm^{-1} occurred due to the presence of primary, secondary and tertiary alcohols, phenols, ethers and esters showing C–O stretching and O–H deformation vibrations. These bands decreased with activation process as compared to the raw material. This situation may be attributed to the decomposition of cellulose, hemicellulose and lignin in the olive-waste cake by chemical ($ZnCl_2$) activation process [12,20,36].

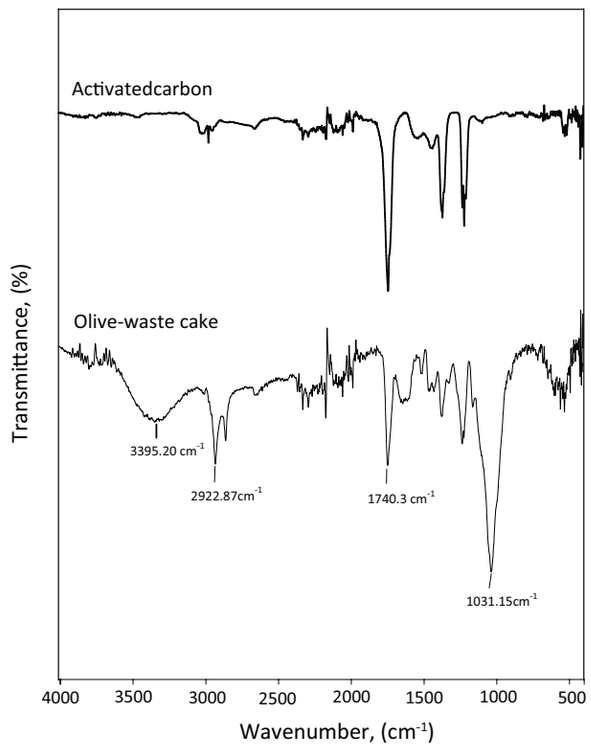

Fig. 1. FTIR spectra of olive-waste cake and activated carbon.

In order to examine the surface morphology, the olive-waste cake and activated carbon were submitted to scanning electron microscopy (SEM). Fig. 2 illustrates the SEM images of the olive-waste cake and activated carbon. The significant differences were observed between the surface topographies of olive-waste cake and activated carbons. It is seen that a thick wall structure of the olive-waste cake exists along with a little porosity at the raw material. This is supported by the BET surface area result (not detected). The thick wall in the raw material opened and wider porosity was created by the chemical activation. Also, activated carbon exhibit an even, homogeneous, highly porous and well pronounced structures, indicating good possibility for the adsorption of pollutions [20,25].

3.2. Effect of initial pH

The initial pH of solution is one of the most important factors influencing the properties of adsorbate, adsorbent and the adsorption process. The influence of initial pH was attributed to the electrostatic interaction between the 2,4-D and the activated carbon surface. The effect of initial pH value on the removal of pesticide (2,4-D) was investigated at the different pH values (2.0, 3.0, 5.0, 6.22, 9.0 and 11.0) for activated carbon (Fig. 3). As shown in Fig. 3, closer rates of 2,4-D removal were observed at pH values 2, 3 and 6.22 (98.31 wt.%; 98.34 wt.% and 98.16 wt.%, respectively) however the rate was lower at pH 5 (97.48 wt.%). The rate of removal decreased continuously over pH 6.22 and finally it reached to minimum value at pH 11 (94.21%), It was

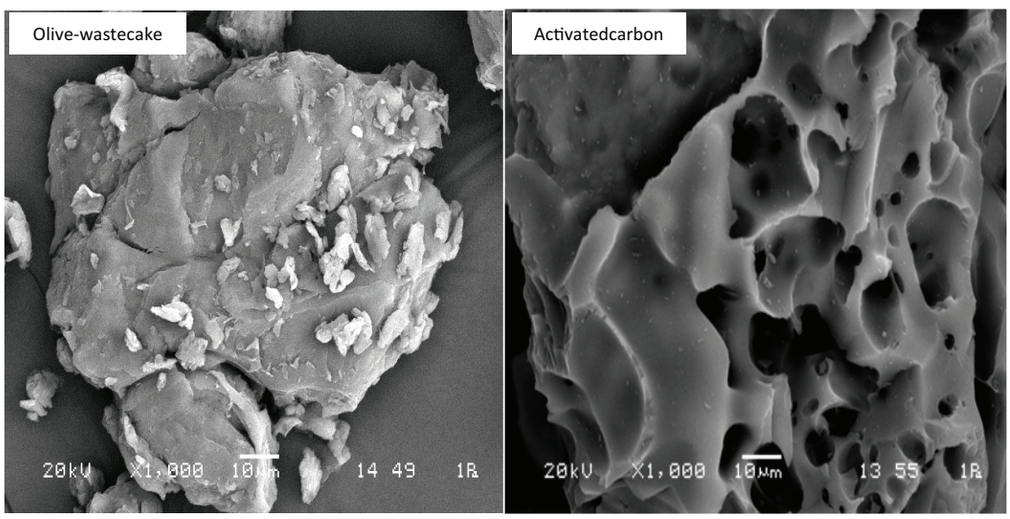

Fig. 2. Scanning electron microscopy images (×1000) of olive-waste cake and activated carbon.

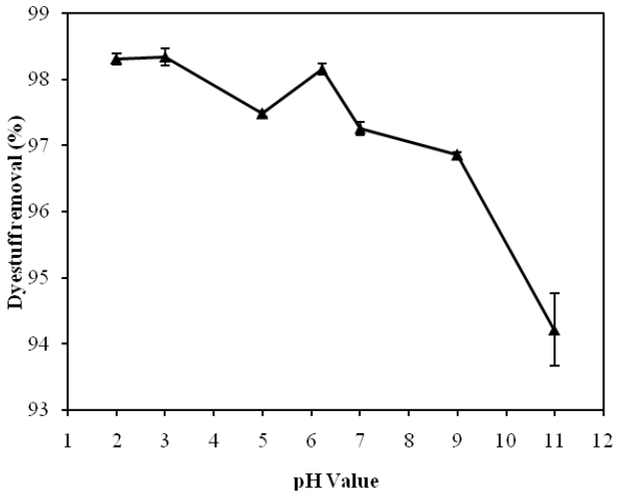

Fig. 3. Effect of solution pH on the adsorption of 2,4-D onto activated carbon.

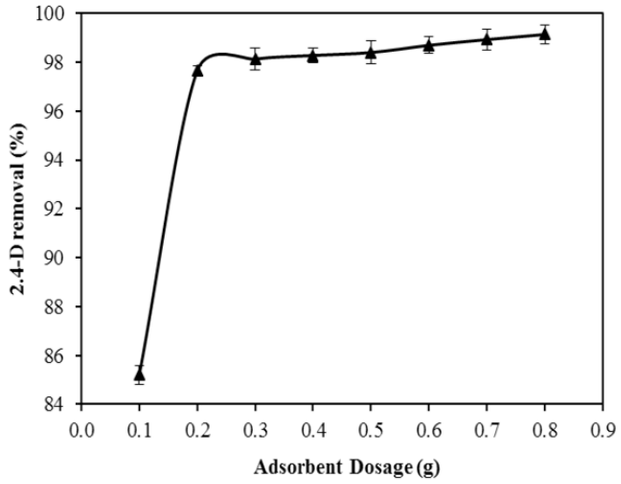

Fig. 4. Effect of adsorbent dosage on the adsorption of 2,4-D onto activated carbon.

observed that the 2,4-D adsorption was highly dependent on the pH of the solution. Solubility of 2,4-D in water is lower than 900 mg/L, and 2,4-D is an acidic chemical substance which is present as deprotonated form (anion) in water solution. Its solubility is even poorer in acid solution which may lead to removal of 2,4-D at high efficiency. On the other hand, the 2,4-D molecules are in the ionized form when the pH value of solution is higher than 6.22, and the degree of dissociation of 2,4-D increases gradually with increasing pH which makes it more negatively charged. On the other hand in alkaline solution the surface charge is negative and 2,4-D is in anionic form and therefore due to the electrostatic repulsion between 2,4-D anion and negative surface, the removal percentage is lower in alkaline solutions [1,6]. Thus pH 6.22 (original value) was selected as the optimum pH value for all further experiments.

3.3. Effect of adsorbent dosage

The effect of the activated carbon dosage on the removal percentage of 2,4-D is shown in Fig. 4. It is apparent that the removal percentage of 2,4-D increased as the activated carbon dosage was increased. The reason for that was the increase in the number of available adsorption sites arisen from the increasing the adsorbent dosage [37]. The removal of pesticide (2,4-D) at different adsorbent dosages showed that it was highly dependent on the dosage until a certain level as explained by the fact that as the adsorbent content increases, the contact surface offered also increases. The saturation level that corresponds to the maximum rate of pesticide elimination is obtained from an activated carbon content of 0.2 g/100 mL solution. When the activated carbon dosage was 0.2 g/100 mL, the removal percentage of 2,4-D could reach to 97.66% beyond which the removal efficiency is negligible. This can be attributed to electrostatic interactions between the functional groups at the cell surfaces [38]. Therefore, the 0.2 g/100 mL was chosen as the optimum dosage and used for further adsorption experiments.

3.4. Effect of initial concentration

The effect of initial concentration on adsorption was investigated from 50 to 300 mg L^{-1} 2,4-D solution. The amount of adsorbed 2,4-D at equilibrium (q_e) increased from 24.07 to 119.32 mg g^{-1} as the initial 2,4-D concentration was increased from 50 to 300 mg L^{-1}. This was due to the increase in the driving force of the concentration gradient, caused by the increase in the initial 2,4-D concentration.

The adsorption isotherm describes how the adsorption molecules distribute between the liquid phase and the solid phase when the adsorption process reaches an equilibrium state [24]. The analysis of the isotherm data by fitting them to different isotherm models is an important step to find the suitable model that can be used for design purpose [32,39]. In this study, four isotherms models were used for describing the results, namely the Langmuir, Freundlich, Dubinin–Radushkevich (D-R) and Temkin isotherm. Comparison of isotherm models for 2,4-D adsorption onto activated carbon are shown in Fig. 5. Also, the fitting results, i.e. isotherm constants and correlation coefficients are shown in Table 2.

The Langmuir model fitted the experimental data better than other isotherm models, indicating the adsorption of 2,4-D onto the activated carbon tended to monolayer adsorption. The Langmuir represents the equilibrium distribution of adsorbate between the solid and liquid phases [40]. Furthermore, the R^2 values of the four isotherm models descend in the order of: Langmuir > Dubinin–Radushkevich > Temkin > Freundlich. Langmuir isotherm model was established by the two hypotheses. First, adsorbent surface is homogeneous with identical adsorption sites. Second, each adsorption sites can only accommodate an adsorbate molecule [37,39]. Through a comparison of correlation coefficients (R^2) of isotherm models, the Langmuir isotherm model (R^2 = 0.9955) was better. So, the Langmuir isotherm model was the most appropriate to describe the correlation of the experimental data in the concentration range studied.

For the Langmuir adsorption isotherm, one of the essential characteristics could be expressed by dimensionless

constant (R_L) called equilibrium parameter [24]. By processing the above equation, R_L value for investigated pesticide-adsorbent system was found to be between 0.018–0.10 and confirmed that the activated carbon is favorable for the adsorption of 2,4-D under the conditions used in this study.

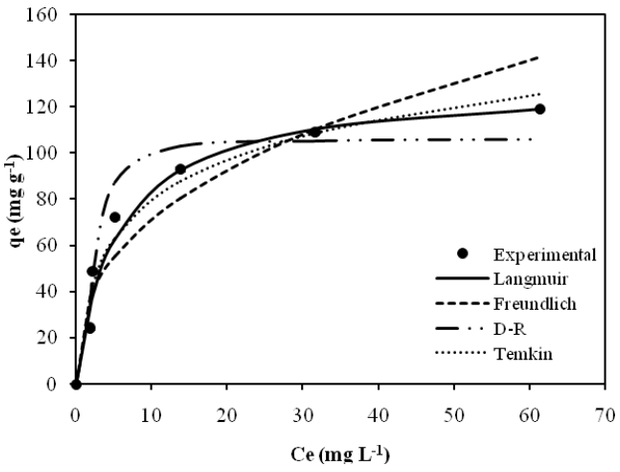

Fig. 5. Comparison of different isotherm models for the adsorption of 2,4-D onto activated carbon.

The Langmuir isotherm parameters, Q_0 and K_L, was found 129.87 mg g^{-1} and 0.181 L mg^{-1}, respectively.

Several studies have been conducted using various types of adsorbents for 2,4-D adsorption. A comparison of the adsorption results of activated carbon obtained in this study with those of some other adsorbents reported in literature is given in Table 3. It can be seen from the table that olive waste cake based activated carbon shows the comparable adsorption capacity with respect to other adsorbents. This indicates that olive waste cake could be considered as a promising material for the removal of 2,4-D from aqueous solutions.

3.5. Adsorption kinetics

Adsorption kinetic describes the control mechanism of adsorption processes which in turn governs the mass transfer and equilibrium time [41]. The experimental data of 2,4-D adsorption onto activated carbon at different time intervals were examined using pseudo-first-order, pseudo-second-order and intra-particle diffusion kinetic models. The pseudo-first-order model is based on the assumption that the adsorption rate is determined by the number of adsorption sites on the surface of the adsorbent; the pseudo-second-order model is based on the assumption that the adsorption rate is determined by the square of the number of vacant adsorption sites on the surface of the adsorbent [1,6,37–40]. The fit of these models was checked by each

Table 2
Adsorption isotherm constants for adsorption of 2,4-D onto activated carbon at 298 K solution temperature

Isotherms	Constants				
Langmuir	Q_o (mg g^{-1})		K_L (L mg^{-1})	R_L	R^2
	129.87		0.181	0.018-0.10	0.9955
Freundlich		K (mg g^{-1})·(L mg^{-1})$^{1/n}$		n	R^2
		29.68		2.64	0.8101
Dubinin-Radushkevich	q_s (mg g^{-1})	B (mol^2 kj^{-2})		E (kj mol^{-1})	R^2
	106.03	1.0		0.707	0.9527
Temkin			A(L g^{-1})	B	R^2
		2.41		25.119	0.9458

Table 3
Comparison of adsorption capacities of 2,4-D onto activated carbons obtained from various materials

Adsorbents	BET Surface Area (m^2 g^{-1})	Adsorption Capacity (mg g^{-1})	Reference
Olive waste cake activated carbon	1418	129.87	Present study
Mesoporous carbon (Fe/OMC)	1054.50	300.42	Tang et al., 2015 [1]
Commercial activated carbon	731.48	181.82	Salman and Hameed, 2010 [2]
Date stones activated carbon	763.40	238.10	Hameed et al., 2009 [5]
Filter paper activated carbon	–	77.13	Khoshnood and Azizian, 2012 [6]
Modified activated carbon	790	47.39	Chingombe et al., 2006 [7]
Fertilizer plant waste activated carbon	380	212.10	Gupta et al., 2006 [8]
Corncob activated carbon	1273.91	300.17	Njoku and Hameed, 2011 [9]
Synthesized Carbon-SBA-15	771	140.05	Momćilović et al., 2013 [10]

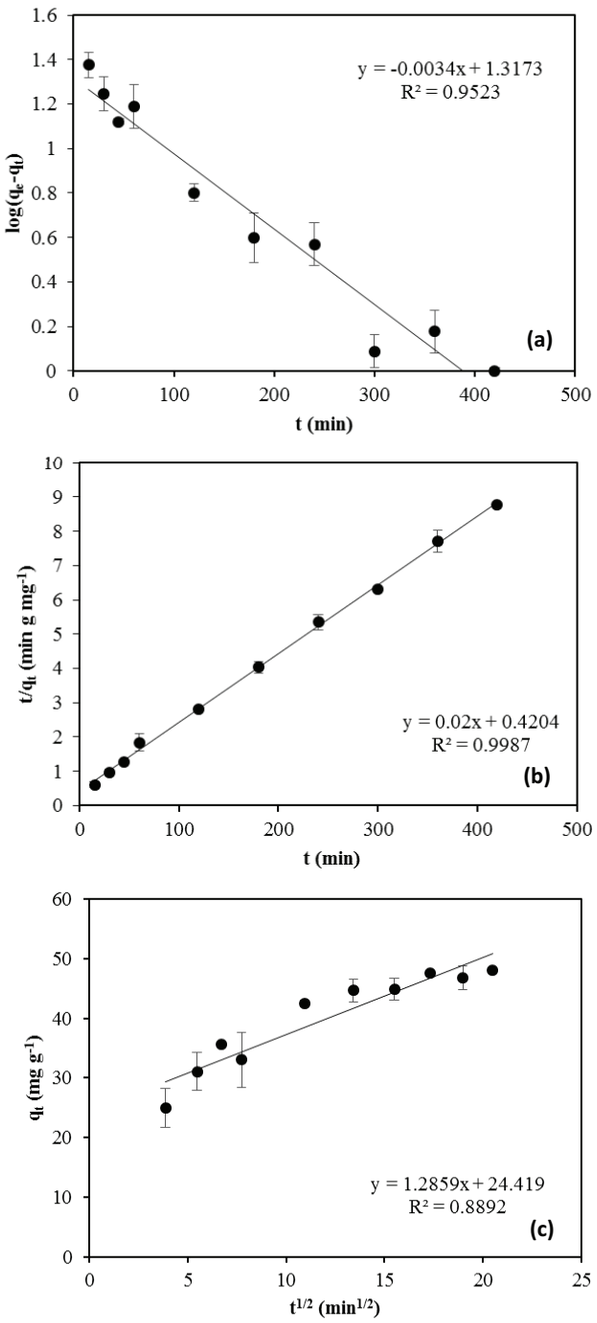

Fig. 6. Linear kinetic plots for the adsorption of 2,4-D onto activated carbon (a) pseudo-first-order, (b) pseudo-second-order, (c) intra-particle diffusion model.

linear plot of log (q_e–q_t) versus t (Fig. 6a), (t/qt) versus t (Fig. 6b) and q_t versus $t^{1/2}$ (Fig. 6c) at 298 K solution temperature, respectively and by comparing to the correlation coefficients for each expression. The rate constants, calculated equilibrium uptakes and the corresponding correlation coefficients are given in Table 4. It was found that the correlation coefficients (R^2 = 0.9987) of pseudo-second-order kinetic model was very close to 1. It means that the adsorption kinetics of 2,4-D on activated carbon was primarily elaborated by the pseudo-second-order kinetic model. In addition, the uniformity between the experimental values of equilibrium adsorption capacity (q_e) and the theoretical values proved that the adsorption experiment was well fitted by t pseudo-second-order kinetic model once again. The result suggested the adsorption rate was closely related to the effective number of adsorption sites of activated carbon prepared from olive-waste cake rather than the concentration of 2,4-D. Therefore the adsorption kinetic could well be approximated more favorably by pseudo-second-order kinetic model for 2,4-D adsorption. Similar results were also reported by other researchers [1–6,37–41]. Maximum adsorption capacity of 2,4-D onto activated carbon was observed at 300 min, it can be said that beyond which there is almost no further increase in the adsorption and in thus selected as the equilibrium contact time.

Table 4
Kinetic parameters for the adsorption of 2,4-D onto activated carbon at 298 K solution temperature.

$q_{e,experimetal}$ (mg g^{-1})		48.828
Pseudo-first-order	k_1 (min^{-1})	0.0078
	$q_{e,calculation}$ (mg g^{-1})	20.76
	R^2	0.9523
Pseudo-second-order	k_2 (g mg^{-1}min^{-1})	0.0475
	$q_{e,calculation}$ (mg g^{-1})	50.00
	R^2	0.9987
Intra-particle diffusion	k_p (mg g^{-1}min$^{-1/2}$)	1.286
	C (mg g^{-1})	24.42
	R^2	0.8892

The pseudo-first-order and pseudo-second-order kinetic models cannot identify the diffusion mechanism and the kinetic results were then analyzed by using the intra-particle diffusion kinetic model [11,29–31]. According to the intra-particle-diffusion model, a plot of q_t versus $t^{1/2}$ should be linear if intra-particle-diffusion is involved in the adsorption process, and if this line passes through the origin the intra-particle diffusion is the rate controlling step. When the plot does not pass through the origin, this is an indication of some degree of boundary layer control and this further shows that the intra-particle diffusion is not the only rate limiting step, but also other kinetic models may control the rate of adsorption, all of which may be operating simultaneously [27,31]. As can be seen from Fig. 6c, the linear plots did not pass through the origin. This indicates that the intra-particle diffusion was not only a rate controlling step.

3.6. Thermodynamic parameters

Adsorption thermodynamics such as Gibbs free energy change ($\Delta G°$), enthalpy change ($\Delta H°$), and entropy change ($\Delta S°$) provide an insight into the mechanism and adsorption behavior of an isolated system. Its original concept assumes that energy cannot be gained or lost, which entropy change is the driving force [32]. Generally, free energy ($\Delta G°$) values between –20 kJ mol^{-1} and 0 kJ mol^{-1} suggests a physisorption

Table 5
Thermodynamic parameters for the adsorption of 2,4-D onto activated carbon

T (K)	$\Delta G°$ (kJ mol^{-1})	$\Delta H°$ (kJ mol^{-1})	$\Delta S°$ (J mol^{-1} K^{-1})
298	– 8.50±0.09	– 19.54±4.08	– 36.96±13.67
308	– 8.08±0.12		
318	– 7.76±0.37		

process; whilst $\Delta G°$ values in range of –80 kJ mol^{-1} to –400 kJ mol^{-1} suggests a chemisorption process [12,29]. In Table 5, the Gibbs free energy change (–8.50, –8.08 and –7.76 kJ mol^{-1}) during the adsorption process was negative for the experimental range of temperatures, corresponding to a spontaneous physical process of 2,4-D adsorption onto activated carbon at 298, 308 and 318 K. The negative value of $\Delta H°$ (–19.54 kJ mol^{-1}) indicates exothermic nature of adsorption process. Meanwhile, the value of $\Delta S°$ was –36.96 J mol^{-1} K^{-1}, which indicated increased randomness at the solid-solution interface with the loading of 2,4-D molecules onto the external and internal surfaces of the carbonaceous substance.

4. Conclusions

This study was demonstrated that activated carbon obtained from olive-waste cake by chemical activation acts as a good adsorbent for the removal of pesticides (2,4-dichlorophenoxyacetic acid) from aqueous solutions. The activated carbon obtained from olive-waste cake by chemical activation ($ZnCl_2$) has high pore volume and a large surface area. It was found that specific surface area and total pore volume of activated carbon were 1418.0 m^2 g^{-1} and 0.410 cm^3 g^{-1}. The surface functional groups and surface morphology of activated carbon were investigated by using FTIR spectrometer and scanning electron microscopy (SEM) techniques. The batch adsorption studies clearly suggest that the high adsorption capacity (129.87 mg g^{-1}) of activated carbon in neutral solutions (pH around 6.22) is due to the strong electrostatic interactions between its adsorption site and pesticide (2,4-D). The optimum adsorbent dosage was determined as 0.2 g/100 mL because of the 2,4-D removal efficiency is negligible at higher adsorbent dosages. The adsorption isotherm studies showed that Langmuir adsorption isotherm model adequately described the adsorption of 2,4-D onto activated carbon and the maximum adsorption capacity was found to be 129.87 mg g^{-1}. In addition, 2,4-D adsorption onto activated carbon follows the pseudo-second-order kinetic model and it has also been applied to predict the rate constant and capacity of adsorption. The thermodynamic parameters indicated a feasible, spontaneous and exothermic adsorption.

Acknowledgement

This work was partial supported by Sakarya University Scientific Research Foundation (Project number: 2016-50-01-001).We thank to our diploma project students for their support during experimental studies.

References

[1] L. Tang, S. Zhang, G.M. Zeng, Y. Zhang, G.D. Yang, J. Chen, J.J. Wang, J.J. Wang, Y.Y. Zhou, Y.C. Deng, Rapid adsorption of 2,4-dichlorophenoxyacetic acid by iron oxide nanoparticles-doped carboxylic ordered mesoporous carbon, J. Colloid. Int. Sci., 445 (2015) 1–8.
[2] J.M. Salman, B.H. Hameed, Adsorption of 2,4-dichlorophenoxyacetic acid and carbofuran pesticides onto granular activated carbon, Desalination, 256 (2010) 129–135.
[3] Z. Aksu, E. Kabasakal, Batch adsorption of 2,4-dichlorophenoxy-acetic acid (2,4-D) from aqueous solution by granular activated carbon, Separ. Purif. Tech., 35 (2004) 223–240.
[4] E. Ayranci, N. Hoda, Studies on removal of metribuzin, bromacil, 2,4-d and atrazine from water by adsorption on high area carbon cloth, J. Hazard. Mater., B112 (2004) 163–168.
[5] B.H. Hameed, J.M. Salman, A.L. Ahmad, Adsorption isotherm and kinetic modeling of 2,4-D pesticide on activated carbon derived from date stones, J. Hazard. Mater., 163 (2009) 121–128.
[6] M. Khoshnood, S. Azizian, Adsorption of 2,4-dichlorophenoxyacetic acid pesticide by graphitic carbon nanostructures prepared from biomasses, J. Ind. Eng. Chem., 18 (2012) 1796–1800.
[7] P. Chingombe, B. Saha, R.J. Wakeman, Effect of surface modification of an engineered activated carbon on the sorption of 2,4-dichlorophenoxy acetic acid and benazolin from water, Metribuzin removal with electro-activated granular carbon, J. Colloid. Int. Sci., 297 (2006) 434–442.
[8] V.K. Gupta, I. Ali, Suhas, V.K. Saini, Adsorption of 2,4-D and carbofuran pesticides using fertilizer and steel industry wastes, J. Colloid. Inter. Sci., 299 (2006) 556–563.
[9] V.O. Njokua, B.H. Hameed, Preparation and characterization of activated carbon from corncob by chemical activation with H_3PO_4 for 2,4-dichlorophenoxyacetic acid adsorption, Chem. Eng. J., 173 (2011) 391–399.
[10] M.Z. Momćilović, M.S. Ranđelović, A.R. Zarubica, A.E. Onjia, M. Kokunešoski, B.Z. Matović, SBA-15 templated mesoporous carbons for 2,4-dichlorophenoxyaceticacid removal, Chem. Eng. J., 220 (2013) 276–283.
[11] Ö. Gerçel, A. Özcan, A.S. Özcan, H.F. Gerçel, Preparation of activated carbon from a renewable bio-plant of Euphorbia rigida by H_2SO_4 activation and its adsorption behavior in aqueous solutions, Appl. Surf. Sci., 253 (2007) 4843–4852.
[12] D. Angin, Utilization of activated carbon produced from fruit juice industry solid waste for the adsorption of Yellow 18 from aqueous solutions, Bioresour. Technol., 168 (2014) 259–266.
[13] K. Mahapatra, D.S. Ramteke, L.J. Paliwal, Production of activated carbon from sludge of food processing industry under controlled pyrolysis and its application for methylene blue removal, J. Anal. Appl. Pyrol., 95 (2012) 79–86.
[14] L. Benammar, T. Menasria, A. Ayachi, M. Benounis, Phosphate removal using aerobic bacterial consortium and pure cultures isolated from activated sludge, Proces. Safety. Environ. Protec., 95 (2015) 237–246.
[15] W.P. Cheng, W. Gao, X. Cui, J.H. Ma, R.F. Li, Phenol adsorption equilibrium and kinetics on zeolite X/activated carbon composite, J. Taiwan. Inst. Chem. Eng., 62 (2016) 192–198.
[16] B. Chen, Z. Chen, Sorption of naphthalene and 1-naphthol by biochars of orange peels with different pyrolytic temperatures, Chemosp., 76 (2009) 127–133.
[17] D. Angin, Production and characterization of activated carbon from sour cherry stones by zinc chloride, Fuel, 115 (2014) 804–811.
[18] M.E. Fernandez, G.V. Nunell, P.R. Bonelli, A.L. Cukierman, Activated carbon developed from orange peels: Batch and dynamic competitive adsorption of basic dyes, Ind. Crop. Prod., 62 (2014) 437–445.
[19] M.J. Ahmed, S.K. Theydan, Physical and chemical characteristics of activated carbon prepared by pyrolysis of chemically treated date stones and its ability to absorb organics, Pow. Technol., 229 (2012) 237–245.
[20] I. Ozdemir, M. Şahin, R. Orhan, M. Erdem, Preparation and characterization of activated carbon from grape stalk by zinc chloride activation, Fuel. Proces. Tech., 125 (2014) 200–206.

[21] J.N. Sahu, J. Acharya, B.C. Meikap, Optimization of production conditions for activated carbons from tamarind wood by zinc chloride using response surface methodology, Biores. Technol., 101 (2010) 1974–1982.
[22] J. Fernández-Bolaños, G. Rodríguez, R. Rodríguez, R. Guillén, A. Jiménez, Extraction of interesting organic compounds from olive oil waste, Grasas. Y. Aceites., 57 (2006) 95–106.
[23] A.S. Erses Yay, H.V. Oral, T.T. Onay, O. Yenigün, A study on olive oil mill wastewater management in Turkey: A questionnaire and experimental approach, Resour. Conserv. Recyc., 60 (2012) 64–71.
[24] J. Yang, K. Qui, Preparation of activated carbons from walnut shells via vacuum chemical activation and their application for methylene blue removal, Chem. Eng. J., 165 (2010) 209–217.
[25] K.Y. Foo, B.H. Hameed, Adsorption characteristics of industrial solid waste derived activated carbon prepared by microwave heating for methylene blue, Fuel. Process. Technol., 99 (2012) 103–109.
[26] A. Mittal, D. Kaur, J. Mittal, Batch and bulk removal of a triarylmethane dye, Fast Green FCF, from wastewater by adsorption over waste materials, J. Hazard. Mater., 163 (2009) 568–577.
[27] P. Senthil Kumar, S. Ramalingam, C. Senthamarai, M. Niranjanaa, P. Vijayalakshmi, S. Sivanesan, Adsorption of dye from aqueous solution by cashew nut shell: Studies on equilibrium isotherm, kinetics and thermodynamics of interactions, Desalination, 261 (2010) 52–60.
[28] H. Demiral, İ. Demiral, F. Tümsek, B. Karabacakoğlu, Pore structure of activated carbon prepared from hazelnut bagasse by chemical activation, Surf. Inter. Anal., 40 (2008) 616–619.
[29] W.Y. Huang, D. Li, Z.Q. Liu, Q. Tao, Y. Zhu, J. Yang, Y.M. Zhang, Kinetics, isotherm, thermodynamic, and adsorption mechanism studies of $La(OH)_3$-modified exfoliated vermiculites as highly efficient phosphate adsorbents, Chem. Eng. J., 236 (2014) 191–201.
[30] D. Angın, T.E. Köse, U. Selengil, Production and characterization of activated carbon prepared from safflower seed cake biochar and its ability to absorb reactive dyestuff, Appl. Surf. Sci., 280 (2013) 705–710.
[31] H. Demiral, G. Gündüzoğlu, Removal of nitrate from aqueous solutions by activated carbon prepared from sugar beet bagasse, Bioreso. Technol., 101 (2010) 1675–1680.
[32] L. Lin, S.R. Zhai, Z.Y. Xiao, Y. Song, Q.D. An, X.W. Song, Dye adsorption of mesoporous activated carbons produced from NaOH-pretreated rice husks, Biores. Technol., 136 (2013) 437–443.
[33] A. Aygün, S. Yenisoy-Karakaş, I. Duman, Production of granular activated carbon from fruit stones and nutshells and evaluation of their physical, chemical and adsorption properties, Micropor. Mesopor. Mater., 66 (2003) 189–195.
[34] V. Gomez-Serrano, J. Pastor-Villegas, A. Perez-Florindo, C. Duran-Valle, C. Valenzuela-Calahorro, FT-IR study of rockrose and of char and activated carbon, J. Anal. Appl. Pyrol., 36 (1996) 71–80.
[35] E. Altintig, S. Kirkil, Preparation and properties of Ag-coated activated carbon nanocomposites produced from wild chestnut shell by $ZnCl_2$ activation, J. Taiw. Ins. Chem. Eng., 63 (2016) 180–188.
[36] M. Inyang, B. Gao, P. Pullammanappallil, W. Ding, A.R. Zimmerman, Biochar from anaerobically digested sugarcane bagasse, Biores. Technol., 101 (2010) 8868–8872.
[37] L. Wang, J. Zhang, R. Zhao, C. Li, Y. Li, C. Zhang, Adsorption of basic dyes on activated carbon prepared from Polygonum orientale Linn: Equilibrium, kinetic and thermodynamic studies, Desalination, 254 (2010) 68–74.
[38] K.W. Goyne, J. Chorover, A.R. Zimmerman, S. Komarneni, S.L. Brantley, Influence of mesoporosity on the sorption of 2,4-dichlorophenoxyacetic acid onto alumina and silica, J. Colloid. Int. Sci., 272 (2004) 10–20.
[39] Y. Li, Q. Du, T. Liu, X. Peng, J. Wang, J. Sun, Y. Wang, S. Wu, Z. Wang, Y. Xia, L. Xia, Comparative study of methylene blue dye adsorption onto activated carbon, graphene oxide, and carbon nanotubes, Chem. Eng. Res. Des., 91 (2013) 361–368.
[40] H. Demiral, C. Güngör, Adsorption of copper(II) from aqueous solutions on activated carbon prepared from grape bagasse, J. Clean. Prod., 124 (2016), 103–113.
[41] A.S. Mestre, A.S. Bexiga, M. Proença, M. Andrade, M.L. Pinto, I.Matos, I.M. Fonseca, A.P. Carvalho, Activated carbons from sisal waste by chemical activation with K_2CO_3: Kinetics of paracetamol and ibuprofen removal from aqueous solution, Biores. Technol., 102 (2011) 8253–8260.